

Supporting Information

Effect of Oxalate and Sulfate on Iron-catalyzed Secondary Brown Carbon Formation

Aseel Al Nimer,^{ξ#} Laura Rocha,^{ξ#} Mohammad A. Rahman,^ξ Sergey A. Nizkorodov,[‡] and Hind A. Al-Abadleh^{ξ*}

^ξDepartment of Chemistry and Biochemistry, Wilfrid Laurier University, Waterloo, ON N2L 3C5, Canada

[‡] Department of Chemistry, University of California, Irvine, California 92697, United States

[#] These co-authors contributed equally to the experimental work

Corresponding Author

* Phone: (519)884-0710, ext.2873; Fax: (519)746-0677; e-mail: halabadleh@wlu.ca.

Journal: Environmental Science and Technology

Supplementary Data (14 pages)

Details on Materials and Method	S2
Figure S1	S5
Figure S2	S6
Scheme S1	S7
Equilibrium constants for the acid dissociation and complexation reactions of iron from the database in Visual MINTEQ, v. 3.1	S8
Scheme S2	S10
Scheme S3	S11
Figure S3	S12
Figure S4	S13
References	S14

Details on Materials and Method:

Chemicals. 1,2-benzenediol (catechol, >99%, CAS: 120-80-9, Sigma-Aldrich), 2-methoxyphenol (guaiacol, \geq 98%, CAS: 95-05-1, Sigma-Aldrich), *trans*-butenedioic acid (fumaric acid, \geq 99%, CAS: 110-17-8, Sigma-Aldrich), *trans, trans*-2,4-hexadienedioic acid (muconic acid, 98%, CAS: 3588-17-8, Sigma-Aldrich), oxalic acid dihydrate (\geq 99%, CAS: 6153-56-6, ACS reagent, Sigma-Aldrich), ammonium sulfate (ACS grade, CAS: 7783-20-2, EMD Chemicals), iron(III) chloride hexahydrate (97%, CAS: 10025-77-1, Sigma-Aldrich), and acetonitrile (HPLC grade, 99.9%, BDH). Aqueous phase solutions were prepared by dissolving the chemicals in Milli-Q water (18.5 M Ω cm) with 0.01 M ionic strength (KCl powder, 99.5%, EM Science). Hydrochloric acid (HCl 6 N, Ricca Chemical Company) and sodium hydroxide (NaOH pellets, 99-100%, EMD) were used to adjust the pH of stock solutions. As described below, all experiments with these chemicals were conducted under dark solution conditions by wrapping vials and beakers with aluminum foil in order to prevent competing photo-Fenton processes.

Product mass experiments. For these experiments, the concentration of the organic reagents was 1 mM. This concentration is atmospherically-relevant as it mimics the high solute:solvent ratio in adsorbed water and in aerosols with relatively low aerosol liquid water content. To investigate the effect of pH, experiments were conducted with the initial pH value at either 3 or 5. The final pH after the 2 h reaction was in the range 2.8-3 and 3-4, respectively. The filters were weighed before filtration and after overnight drying. The particles were washed with Milli-Q water several times prior to drying. Each experiment was repeated 3-4 times on clean filters for reproducibility.

HPLC experiments. Chromatograms were collected using a Waters Delta 600 instrument equipped with a Waters 2487 Dual Wavelength Absorbance Detector set at 271 and 337 nm. A Waters in-line degasser as well as helium gas were used for sparging at 20 mL min⁻¹ throughout the experiment to avoid air bubbles. The mobile phase, 95% water and 5% acetonitrile, was filtered and flown isocratically at a flow rate of 1 mL min⁻¹ for experiments with fumarate and muconate. The column was a Hypersil GOLD C8 column (Thermo Scientific, 4.6 x 250 mm), 5 µm particle size, and 175 Å pore size. Under these conditions, elution times for at pH 5 are 2.9 and 3.1 min for fumarate, and muconate, respectively.

For solutions prepared according to *method 1*, data collection started when iron was added, whereas in *method 2*, data collection started when the organic reagent was added. The particle material refractive index (RI) in these experiments was set to 1.6. The following criteria were used in choosing the data points shown in the figures for experiments done using *method 1*: (a) values of polydispersity index (PDI) < 0.5, (b) no multimodal fits in % intensity vs. size plots, (c) in the presence of other peaks, the intensity of minor peaks has to be less than 10% of the most intense peak, and (d) the correlation coefficient fits the model under the tab ‘cumulants fit’.

Dynamic light scattering (DLS) experiments. It is important to note that the DLS measures the hydrodynamic average size of particles formed in solution. This DLS-measured size should not be confused with the size of atmospheric aerosol particles formed during various new particle formation processes.³⁵ The processes described here refer to the formation of insoluble and involatile polymeric materials from soluble components in solution. In the language of atmospheric chemists, these processes contribute to aerosol growth but not to new particle formation. To avoid confusion, the term ‘solution nucleation’ will be used in the interpretation of the DLS data in order to distinguish it from nucleation of new particles in air.

Attenuated total reflection Fourier transform infrared spectroscopy (ATR-FTIR). Particles formed from the reaction of FeCl_3 with fumarate and muconate in the presence of sulfate were deposited onto a ZnSe crystal from a water/ethanol slurry followed by drying overnight. Absorption spectra of these particles were obtained by referencing to the clean and dry ZnSe crystal. The resolution was 8 cm^{-1} and 100 scans were averaged per spectrum. For comparison, the ATR-FTIR absorbance spectrum of 0.5 M ammonium sulfate solution at pH 7 was recorded by referencing to the background solution.

Ion chromatography experiments. These experiments were conducted to verify the consumption of sulfate in the formation of polycatechol particles from catechol solutions containing sulfate. Polycatechol particles were prepared according to *method 2* described above. Instead of filtration, the particle-containing solution was transferred to a centrifuge tube. The supernatant was collected after 30 min centrifugation at 9000 relative centrifuge force (RCF) to remove the particles from solution. The sulfate concentration in the supernatant and in the standard sulfate solution prepared to mix with FeCl_3 and catechol was determined using ion chromatography with conductivity according to a modified EPA 300.1 method by ALS Environmental Labs.

Thermogravimetric and differential scanning calorimetry analysis (TGA/DSC). The TGA analysis was completed on a TGA Q500 V20.13 Build 39 instrument while flowing nitrogen and air at 60 and 40 mL min^{-1} for balance and sample, respectively. The sample was thermally equilibrated at 25°C , followed by a temperature ramp at a rate of $10^\circ\text{C min}^{-1}$ up to 800°C . The DSC analysis was completed on a DSC Q2000 V24.11 Build 124 while flowing nitrogen gas at

50 mL min⁻¹. The sample was thermally equilibrated at 30°C, followed by a temperature ramp at a rate of 5°C min⁻¹ up to 200°C.

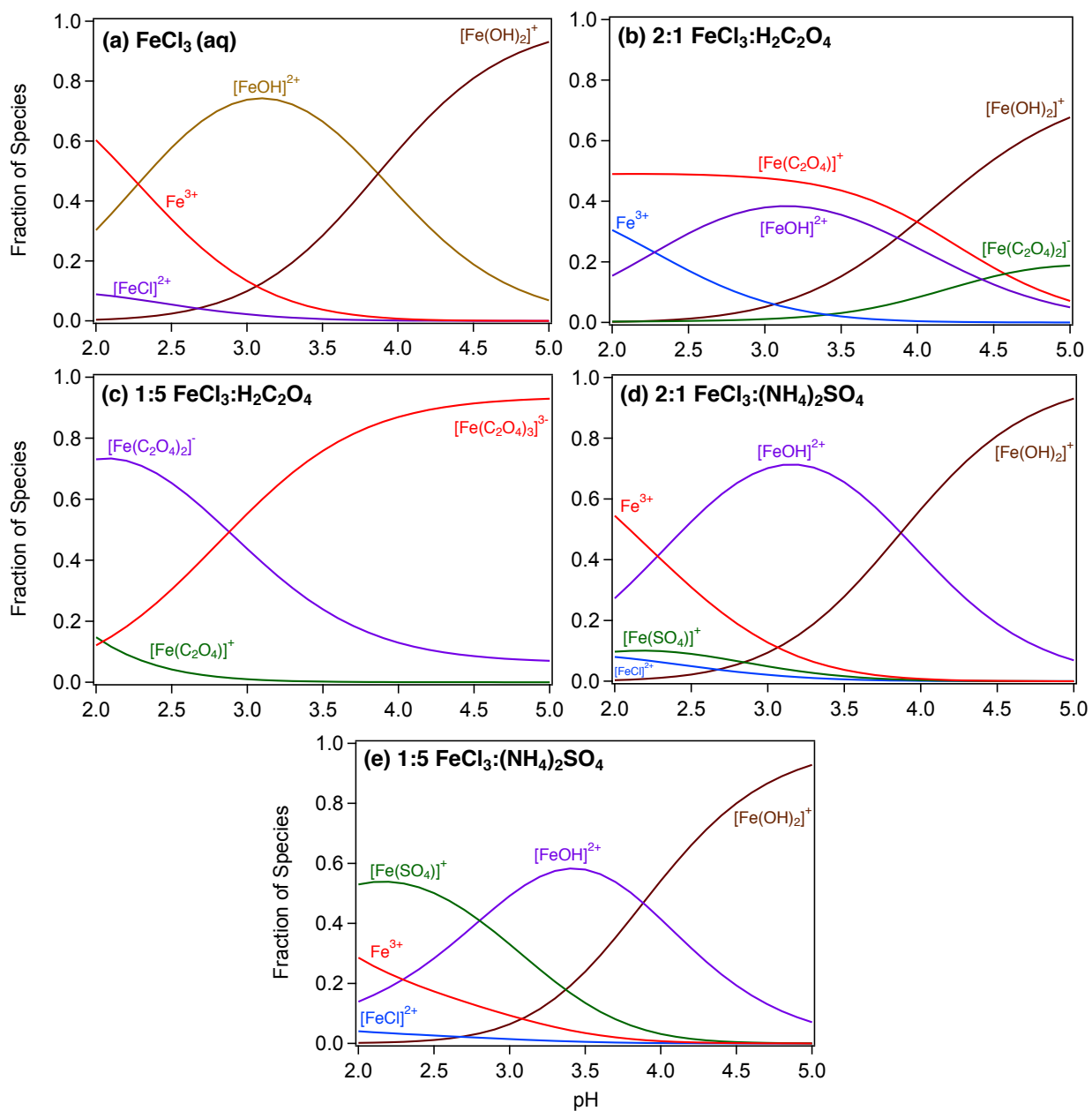


Figure S1. Speciation curves of iron chloride, oxalate, and sulfate with variable molar ratios. Ratios in headings are mol:mol. The curves were generate using equilibrium constants for the acid dissociation and complexation reactions of iron from the database in Visual MINTEQ, v. 3.1.

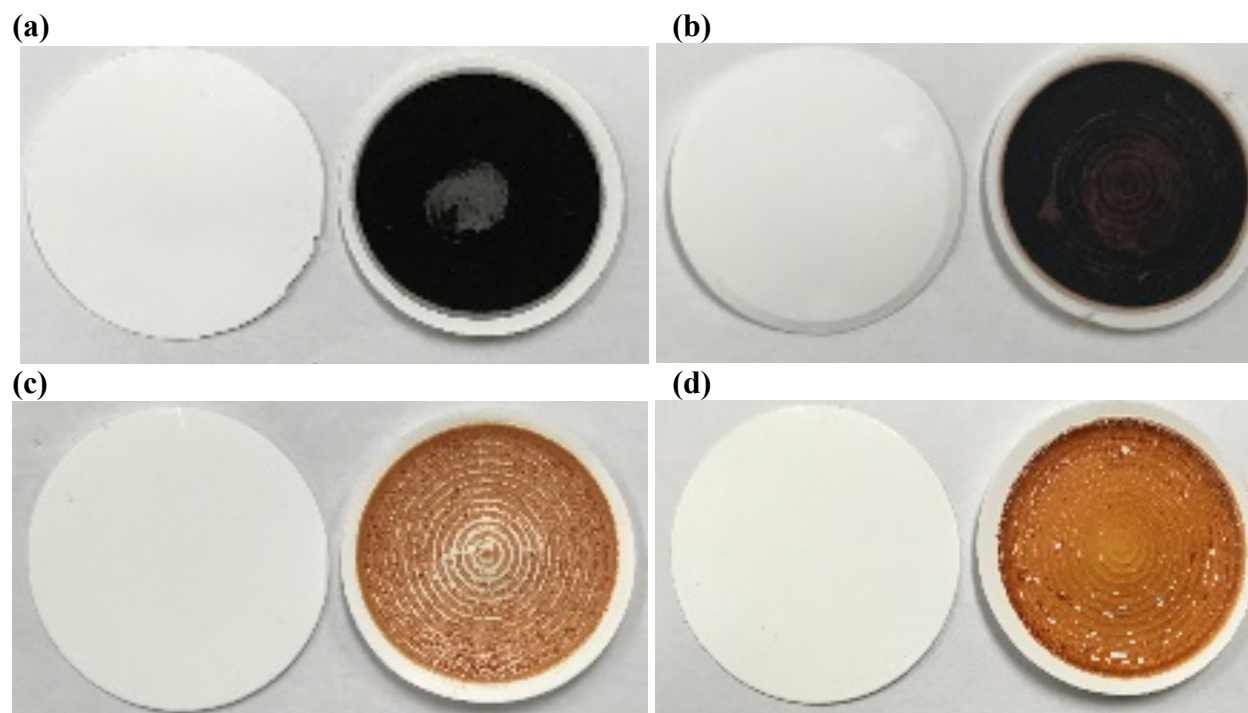
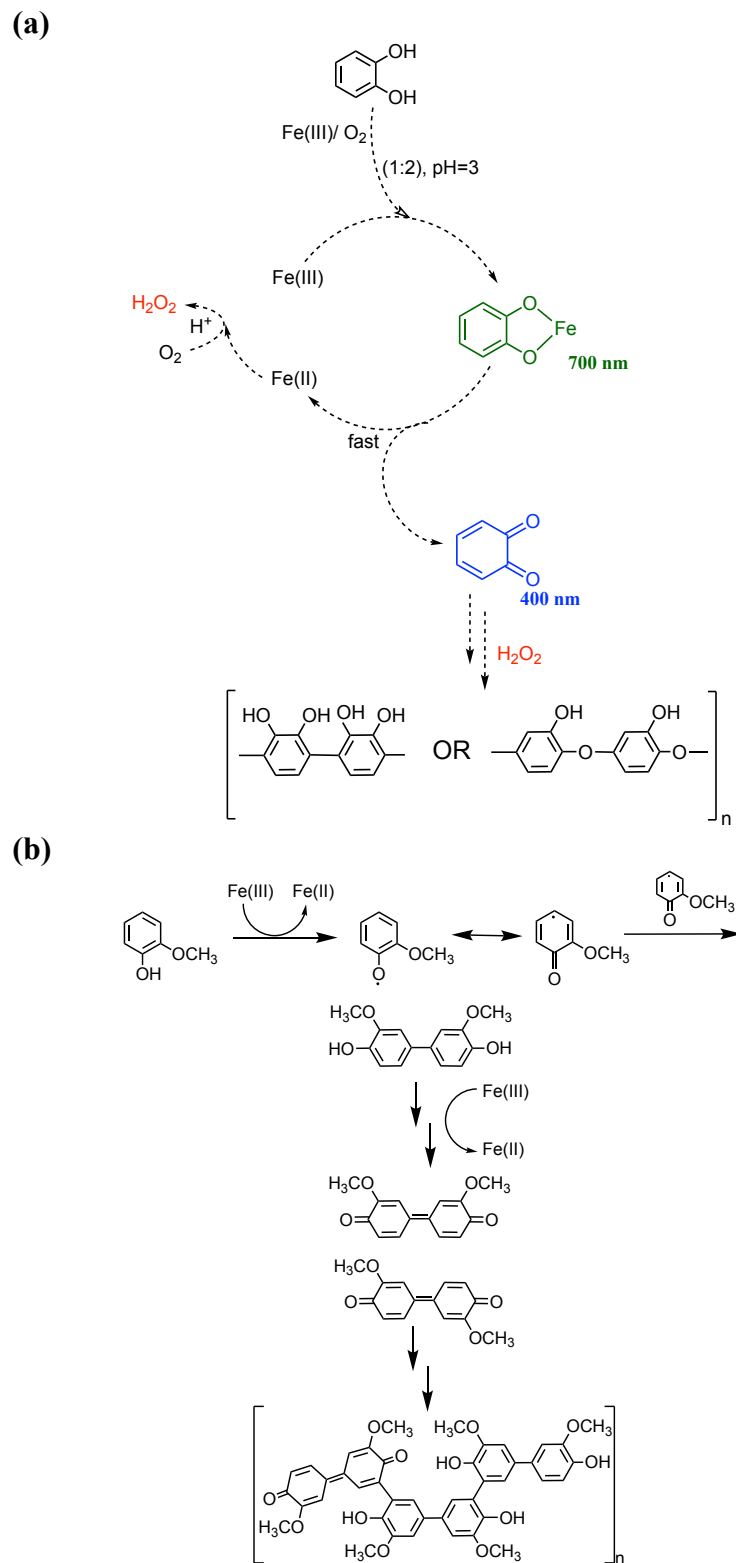
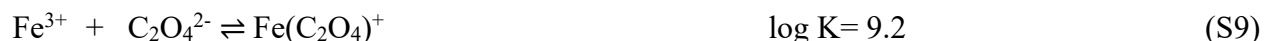
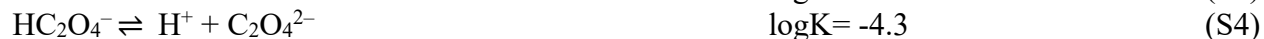
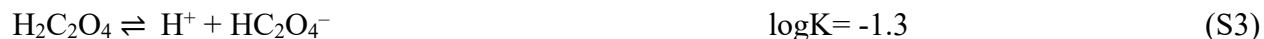


Figure S2. Photographs of filters containing (a) polycatechol, (b) polyguaiacol, (c) Fe-polyfumarate, and (d) Fe-polymuconate following 2 hr reactions according to *method 1*. The reaction solutions contained the following molar ratios - 2:1:1 Fe:catechol (or guaiacol):Oxalate at pH 3, and 2:1:1 Fe:fumarate (or muconate):Oxalate at pH 5.



Scheme S1. Suggested mechanisms for the formation of (a) polycatechol,^{2,3} and (b) polyguaiaicol.⁴⁻⁶

Equilibrium constants for the acid dissociation and complexation reactions of iron from the database in Visual MINTEQ, v. 3.1:



-1 × (S1)+(S12)



-1 × (S1)+(S13)



-1 × (S1)+(S7)+ (S14)



Note: in the presence of excess dissolved iron and dissolved oxygen, iron catalyzes deprotonation of catechol at pH 3, below the first pKa in reaction S5.¹

-1 × (S1)+(S4)+(S9)



(S17) - (S18):



In excess oxalate at pH 3:

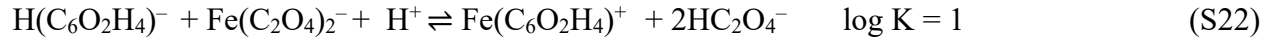
-1 × (S1)+ 2 × (S4) + (S10):



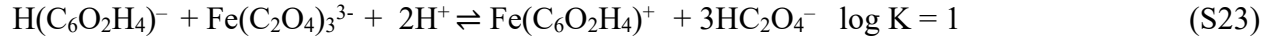
-1 × (S1) + 3 × (S4) + (S11)



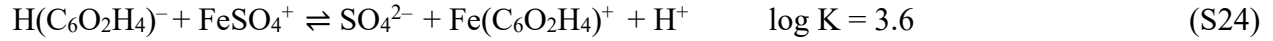
(S17)-(S20):



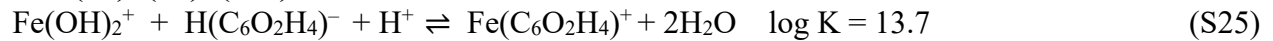
(S17)-(S21):



-1 × (S15)+(S17)



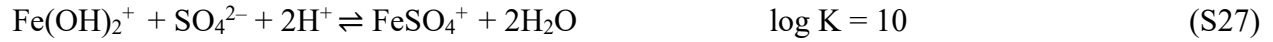
-1 × (S2)+(S7)+(S14)



-1 × (S2)+(S9)



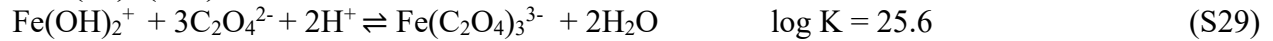
-1 × (S2)+(S12)

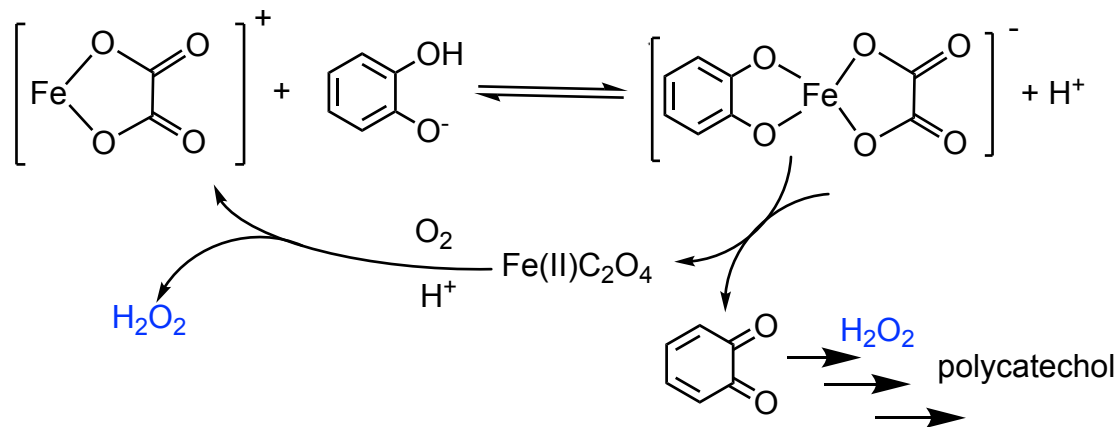


-1 × (S2)+(S10)



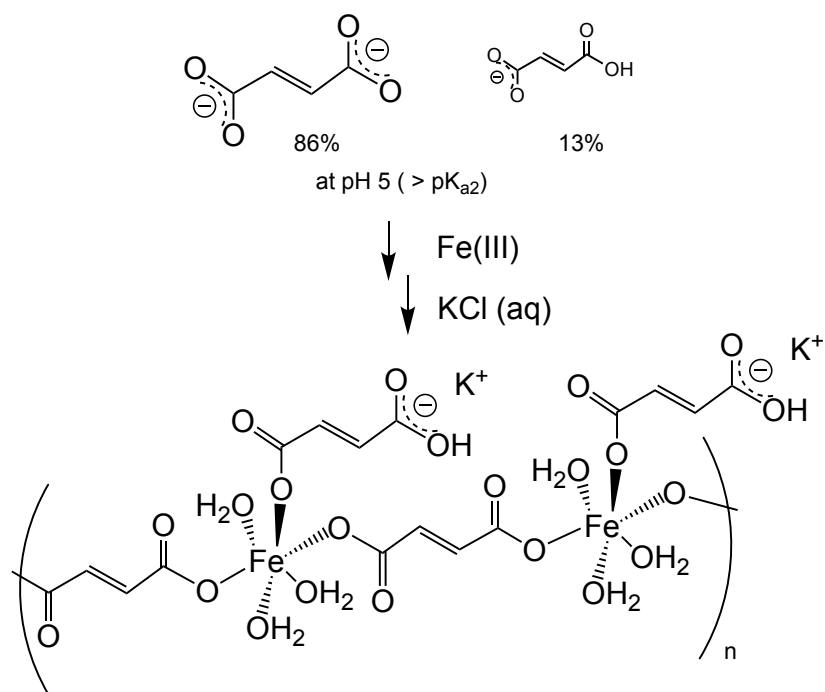
-1 × (S2)+(S11)



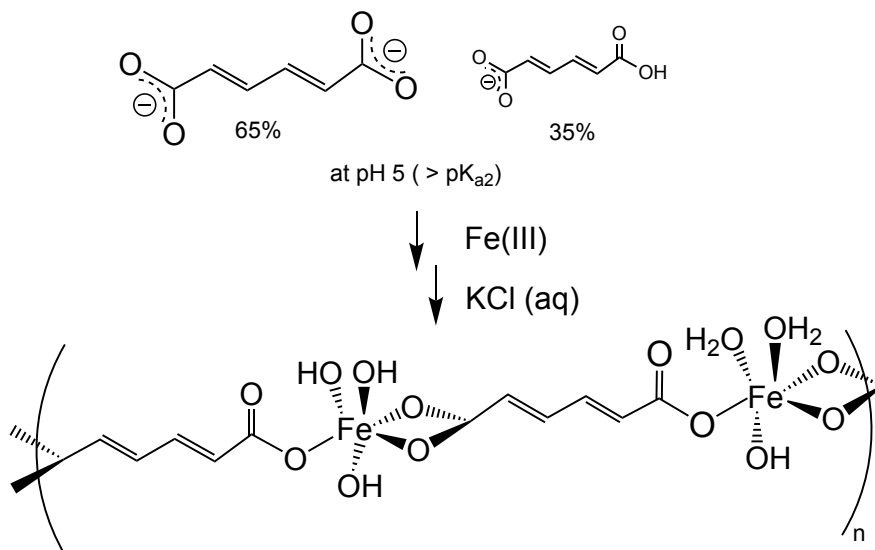


Scheme S2. Suggested mechanism for the formation of polycatechol from the iron oxalate catecholate complex.

(a)



(b)



Scheme S3. Diagrams for the formation of (a) Fe-polyfumarate, and (b) Fe-polymuconate based on structural elucidation of the organometallic polymers in reference.⁷ The percentages show the fraction of species in solution based on the pK_a values of fumaric and muconic acids, respectively.

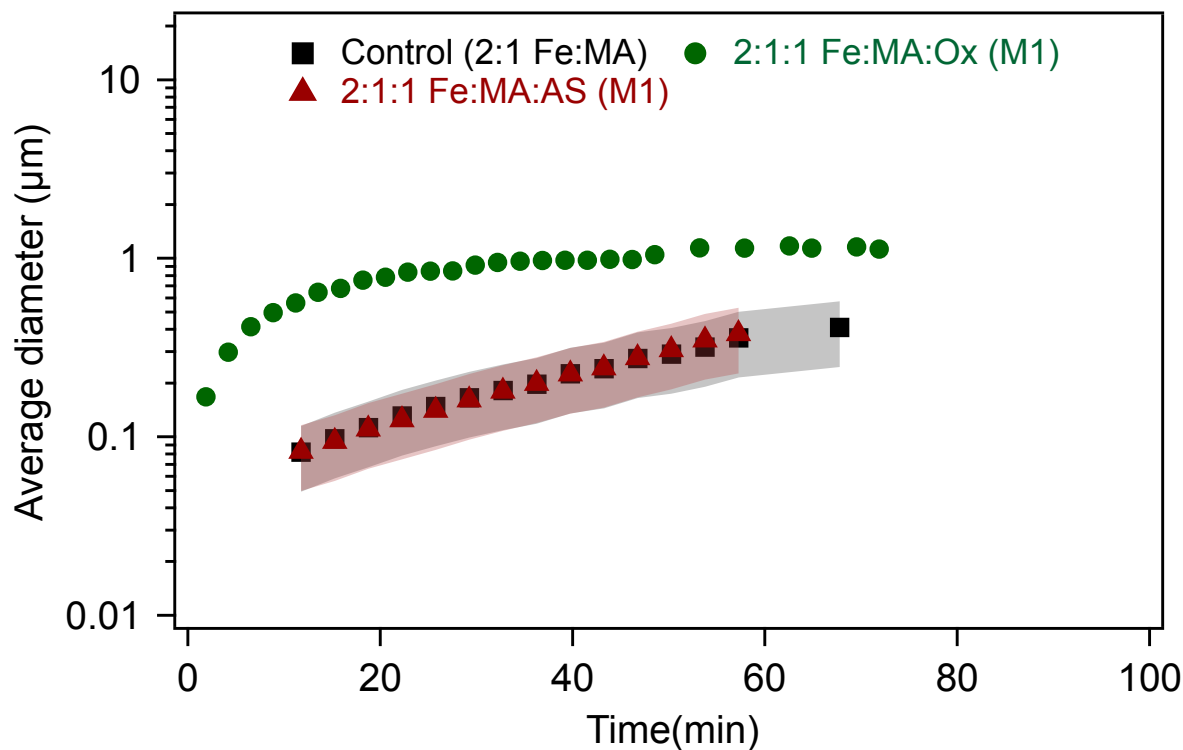


Figure S3. Effect of adding oxalate (Ox) and ammonium sulfate (AS) on particle size from time-dependent DLS measurements during the dark aqueous phase reaction of muconate (25 μM , MA) with FeCl_3 . The molar ratio in parenthesis results in the maximum product mass per data shown in Figure 1. Initial and final solution pH are similar to those in Figure 1, unless indicated otherwise. ‘M1’ stands for *method 1*, where organic reagents were mixed first with AS or Ox, then reaction time started when Fe is added. The shaded areas represent the standard deviation of three trials. Unshaded data represent the average of two trials, with a standard deviation the size of the marker width (15%).

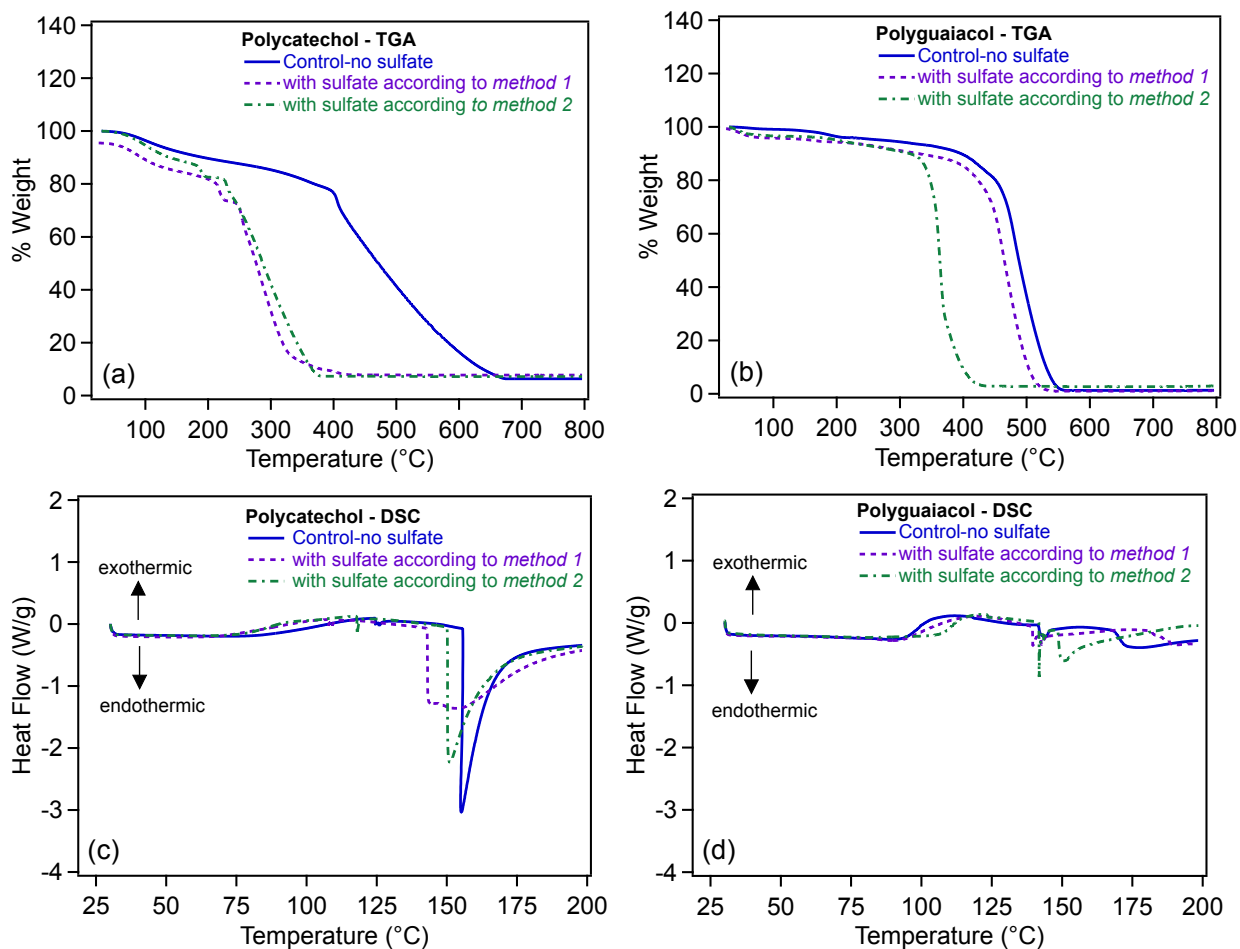


Figure S4. Thermal decomposition and melting of polycatechol (a and c) and polyguaiacol (b and d) particles prepared in solutions without sulfate (control) and with sulfate according to *method 1* or *method 2* at pH 3.

References:

- (1) Perron, N. R.; Brumaghim, J. L., A review of the antioxidant mechanisms of polyphenol compounds related to iron binding. *Cell Biochem. Biophys.* **2009**, *53*, 75-100.
- (2) Slikboer, S.; Grandy, L.; Blair, S. L.; Nizkorodov, S. A.; Smith, R. W.; Al-Abadleh, H. A., Formation of light absorbing soluble secondary organics and insoluble polymeric particles from the dark reaction of catechol and guaiacol with Fe(III). *Environ. Sci. Technol.* **2015**, *49*, 7793-7801.
- (3) Faure, E.; Falentin-Daudre, C.; Jerome, C.; Lyskawa, J.; Fournier, D.; Woisel, P.; Detrembleur, C., Catechols as versatile platforms in polymer chemistry. *Prog. Poly. Sci.* **2013**, *38*, 236-270.
- (4) Hwang, S.; Lee, C.-H.; Ahn, I.-S., Product identification of guaiacol oxidation catalyzed by manganese peroxidase. *J. Ind. Eng. Chem.* **2008**, *14*, 487-492.
- (5) Doerge, D. R.; Divi, R. L.; Churchwell, M. I., Identification of the colored guaiacol oxidation product produced by peroxidases. *Anal. Biochem.* **1997**, *250*, 10-17.
- (6) Crawford, R. L.; Robinson, L. E.; Foster, R. D., Polyguaiacol: A useful model polymer for lignin biodegradation research. *Appl. Environ. Microbiol.* **1981**, *41*, (5), 1112-1116.
- (7) Tran, A.; William, G.; Younus, S.; Ali, N. N.; Blair, S. L.; Nizkorodov, S. A.; Al-Abadleh, H. A., Efficient formation of light-absorbing polymeric nanoparticles from the reaction of soluble Fe(III) with C4 and C6 dicarboxylic acids. *Environ. Sci. Technol.* **2017**, *51*, 9700-9708.